


Article

HKUST-1 Supported on Zirconium Phosphate as an Efficient Catalyst for Solvent Free Oxidation of Cyclohexene: DFT Study

Razia Aman ^{1,2}, Abraham Clearfield ¹, Mohammad Sadiq ^{2,*}  and Zahid Ali ³

¹ Department of Chemistry, Texas A&M University, College Station, TX 77843, USA; razia.aman@yahoo.com (R.A.); clearfield@chem.tamu.edu (A.C.)

² Department of Chemistry, University of Malakand, Chakdara 18800, KP, Pakistan

³ Center for Computational Materials Science, University of Malakand, Chakdara 18800, KP, Pakistan; zahidf82@gmail.com

* Correspondence: sadiq@uom.edu.pk; Tel.: +92-945-763441

Received: 15 October 2018; Accepted: 5 November 2018; Published: 15 November 2018



Abstract: Layer by layer metal-organic framework (MOF) supported on zirconium phosphate (ZrP) was synthesized at very mild conditions and used for the liquid phase oxidation of cyclohexene in solvent free condition in the presence of molecular oxygen. The MOF-ZrP was characterized by X-ray diffractometer (XRD), scanning electron microscope (SEM), thermal gravimetric analyzer (TGA), Fourier-transform infrared spectrometer (FT-IR) and Brunauer-Emmett-Teller (BET) surface area analyzer. The characterization shows a smooth morphology of MOF-ZrP with good stability under 200 °C having surface area 285 m²/g. The catalytic activity of the MOF-ZrP revealed that increase of layers of MOF on ZrP enhances conversion, as well as selectivity of oxidation of cyclohexene. DFT studies were used to explore the structure and electron properties of HKUST-1 (Hong Kong University of Science and Technology), which is a clue for the catalytic behavior of the catalyst.

Keywords: MOF-ZrP; cyclohexene; solvent free

1. Introduction

Oxyfunctionalization of hydrocarbons is a fundamental reaction in organic chemistry and industry. The oxygenated products of hydrocarbons are key intermediates in valued fine chemicals. Especially six-carbon cyclic hydrocarbons, represented by cyclohexane and cyclohexene, give a variety of oxygen-containing products [1]. Hydrocarbons are naturally abundant raw feedstock for petrochemical industries, that occur in reduced form and oxidation is the only way to convert these substances into valued chemicals [2]. For this purpose, a variety of catalysts and oxidants have been utilized to convert HCs into other products, but the oxidation of these substances is not selective. Cyclohexane produces cyclohexanol and cyclohexanone, but these products are more reactive than cyclohexane and oxidize into other products [3]. Similarly, cyclohexene can be oxidized to give allylic oxidation products, such as cyclohexanol and cyclohexanone and can be oxidized at C=C bond to give cyclohexene oxide and other products. Thus, it is still a challenge to enhance the selectivity towards ketone products by designing an efficient catalyst [4]. Many homogeneous catalysts containing redox transition metals like Cu, Co, Fe and Mn can oxidize alkenes with oxygen, but the catalyst separation is difficult in liquid phase reactions. To make the recovery of catalysts easy, homogeneous catalysts are anchored onto solid supports [5]. Heterogeneous catalysts with different dangerous, expensive and explosive oxidants have been reported for oxidation of HCs, that are not acceptable for industries. Therefore, the search for an ecofriendly, cheap and efficient catalytic system with molecular oxygen is never ending. Recently, metal-organic frameworks containing transition metals like Cu, Co, Fe, V, etc., have been reported as

efficient catalysts in oxidation reactions [6]. Liu et al. [7] has reported $\text{Cu}^{2+}@\text{Comoc-4}$ for oxidation of cyclohexene with molecular oxygen. Three major products cyclohexenol, cyclohexenone and cyclohexene oxide were obtained with 49% conversion in 7 h. PVMo/Hmont has been reported for allylic oxidation with hydrogen peroxide. Cyclohexene oxide, cyclohexenol, cyclohexenone and cyclohexanol were produced where the conversion was 98% [8]. Junghans et al. [9] has reported Copper-MOF (metal-organic framework) with triazolyl isophthalate linkers for oxidation of cyclohexene where the three major products were obtained with tertiary butyl hydroperoxide (TBHP) after 7 h. Farzaneh et al. [10] reported Mn-MOF with benzenetricarboxylate (BTC) and dimethylfurane (DMF) for oxidation of different alkanes and alkenes in the presence of TBHP. For cyclohexene, only two products, cyclohexenol and cyclohexenone were obtained. Cyclohexenone was the major product with 75% selectivity while total conversion was 100% in 24 h. HKUST-1 has been used as catalyst for oxidation of trans-ferulic acid to vanillin. After one hour of reaction, the yield of vanillin was 98% in acetonitrile [11]. Copper immobilized within Zr-based MOF with pyridine units (Zr-MOF-bpy- CuBr_2) has been reported as an efficient catalyst for liquid phase epoxidation of cyclooctene in toluene. The %conversion was 88.5% with selectivity of 95.3% when TBHP was used as oxidant after 12 h at 363 K [12]. $\text{Fe}_3\text{O}_4@\text{HKUST-1}$ has been reported for one-pot sequential deacetalization and Knoevenagel condensation reaction. Benzaldehyde dimethylacetal was completely converted into benzylidenemalononitrile through the formation of benzaldehyde in 5 h at 363 K in the presence of 1,4-dioxane. Similarly, Pd/ $\text{Fe}_3\text{O}_4@\text{HKUST-1}$ has been used for hydrogenation of 1-octene with 98% yield of octane within 3 h [13]. Copper incorporated into Zr-based MOF (UiO-66-(COOH)₂) has been reported for oxidation of cyclooctene. Three different salts of copper were utilized for catalysts preparation and tested for their catalytic activity. All the catalysts showed excellent catalytic activity yielding 99% in 4 h at 40 °C [14].

Layered zirconium phosphates are very attractive for materials chemists. The layered structure consists of zirconium atoms lying in a plane and sandwiched by $\text{O}_3\text{P-OH}$ groups situated alternatively above and below the plane. The compound is highly insoluble in strong acidic and alkaline media [15]. Clearfield and Stynes crystallize zirconium phosphate and other Group(IV) metals for the first time in 1964. The general formula for the phosphates is $\text{Zr}(\text{HPO}_4)_2 \cdot \text{H}_2\text{O}$ that possess layered structure. There are different methods for preparation of zirconium phosphate, but very common methods are reflux and direct precipitation. Crystallinity changes with the concentration of acid and reflux time while surface area and surface acidity decrease with increase in concentration of acid and reflux time [16]. Zirconium phosphate is a versatile ion exchanger. Each zirconium atom possesses two protons that can be exchanged by inorganic and organic cations. Clearfield et al. has interesting reports where they have studied the ion exchange behavior of α -ZrP for Na^+ , K^+ and many more metal ions [17].

α -ZrP has been investigated as an acid catalyst and catalyst support for variety of reactions. Zhang et al. reported α -ZrP catalyst for synthesis of stearic acid monoethanolamide where conversion was 92.9% after 12 h of reaction at 120 °C [18]. Clearfield et al. have reported Ag/ α -ZrP catalyst for oxidation of ethylene. The α -ZrP used as support was first exchanged by Na^+ and K^+ ions, where Na^+ exchanged α -ZrP proved much higher catalytic activity as compared to K^+ exchanged α -ZrP [19]. Ebatani et al. investigated a composite catalyst of Pd NPs/ α -ZrP for the synthesis of 1,6-Hexandiol [20]. Panda et al. have investigated Cr(III) ions/ m -ZrP for oxidation of allylic and benzylic compounds to corresponding carbonyl compounds. The catalyst resulted in higher conversions with 100% selectivity [21]. α -ZrP has also been reported as solid support for organo metallic complexes. Fe(Salen) complexes and Cu(Salen) complexes supported on α -ZrP have been reported for oxidation of cyclohexene with peroxides. The catalyst was prepared by a two-step method. Fe(III) and Cu(II) ions were exchanged in α -ZrP to form α -ZrP-Fe(III) and α -ZrP-Cu(II) precursors. Then intercalation of salen into precursors was carried out by flexible ligand technique. The %conversion of cyclohexene was 18.04% and 26.71% respectively, where products were cyclohexenol, cyclohexenone and cyclohexene oxide [22,23].

A problem with MOFs is their low thermal and chemical stability and separation from the reaction mixture. So immobilizing MOFs on the surface of support material is of great interest to make it heterogeneous especially for catalysis.

Herein we report the catalytic activity of HKUST-1 supported on zirconium phosphate in the liquid phase oxidation of cyclohexene in solvent free conditions with molecular oxygen.

2. Results and Discussion

The X-ray diffractometer (XRD) reveals that there is a distinct peak at 10.75° for ZrP. The progressive development of MOF layers on the surface of ZrP gave rise to many new peaks. With four layers of MOF deposition, the peak at 10.75° disappears, which indicates the successive growth of MOF on the surface, as shown in Figure 1a–f. The characteristic peak of ZrP did not shift with the deposition of MOF suggesting that the Cu ions have exchanged only the surface protons and sodium ions from Na-ZrP. In order to prevent the penetration of Cu ions into the inter layers of zirconium phosphate, sodium exchanged ZrP was used as support. There is a distinct peak for MOF at 8.0° with six layers of deposition. Figure 1a–f, shows the microstructure of ZrP and HKUST-1 on the surface of ZrP. With the increase in the layers of HKUST-1, the grain size gradually increased. Initially, a lower concentration of reactants resulted in the formation of a layer of minor HKUST-1 dispersed uniformly over the surface of ZrP. The smooth morphology of HKUST-1/ZrP revealed the retention of shape of parent support material and uniformed growth of HKUST-1 on the surface of ZrP [24].

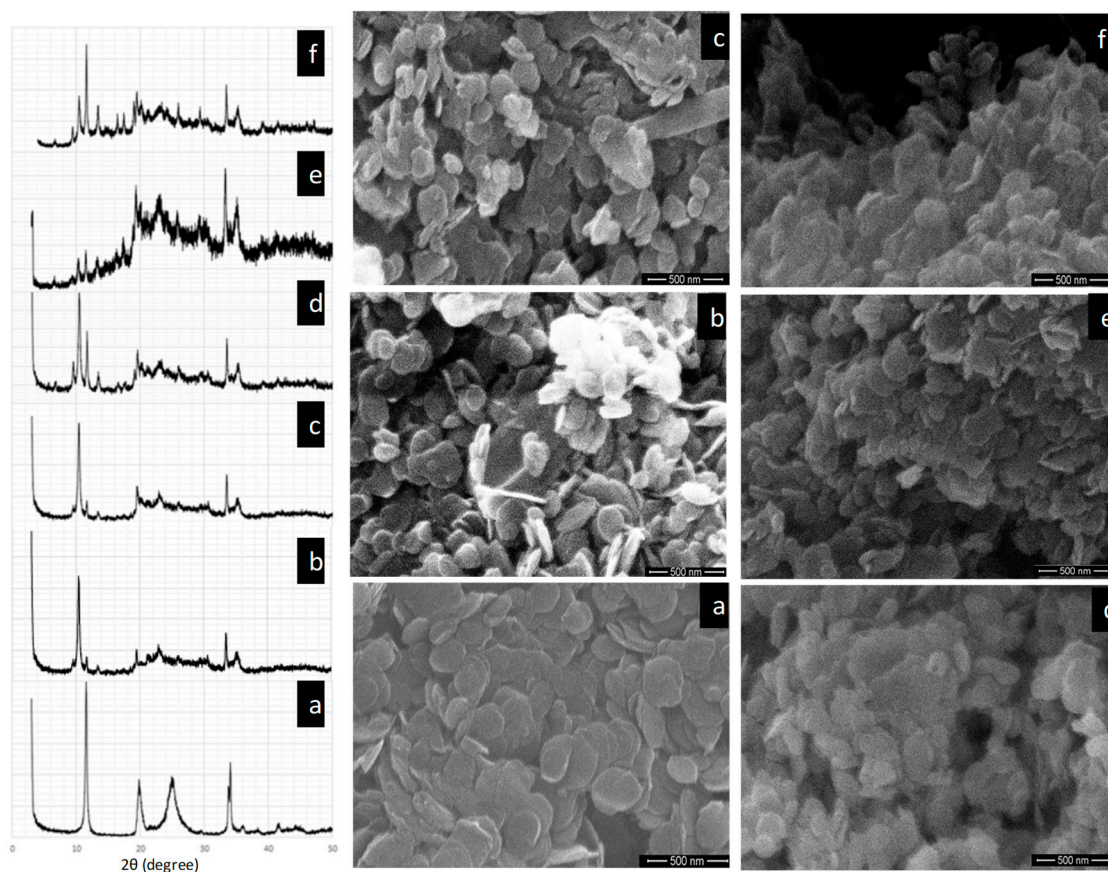


Figure 1. (a) X-ray diffractometer (XRD) pattern and scanning electron microscope (SEM) image of ZrP. (b) XRD pattern and SEM image of metal-organic framework (MOF)-ZrP with two layers. (c) XRD pattern and SEM image of MOF-ZrP with four layers. (d) XRD pattern and SEM image of MOF-ZrP with six layers. (e) XRD pattern and SEM image of MOF-ZrP with eight layers. (f) XRD pattern and SEM image of MOF-ZrP with 10 layers.

TGA curve reveals 12% weight loss with increase in temperature, as shown in Figure 2a. The first weight loss is due to dehydration of the ZrP and residual solvent up to 150 °C. The second weight loss beyond 150 °C to 450 °C is due to the decomposition of ligand. Figure 2b exhibits that two bands at 3595 cm^{-1} and 3502 cm^{-1} are attributed to O-H stretching. The bands at 1624 cm^{-1} and 1215 cm^{-1} are due to the carboxylate group of BTC ligand. The band at 952 cm^{-1} suggests the condensation of P-OH of ZrP. The band at 609 cm^{-1} is due to the vibrations of Zr-O.

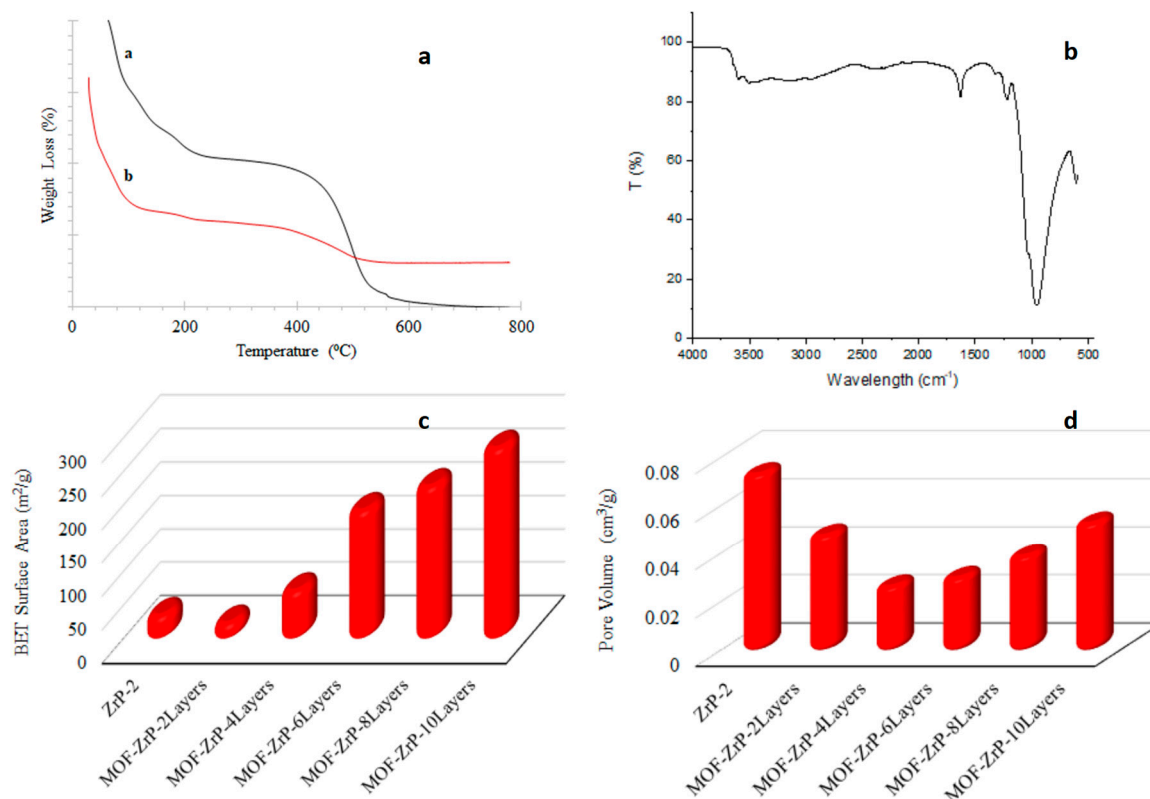


Figure 2. (a) TGA curves of ZrP and MOF-ZrP (a,b). (b) FTIR of MOF-ZrP. (c) BET surface area of ZrP and MOF-ZrP with different layers. (d) Pore Volume of ZrP and MOF-ZrP with different layers.

Figure 2c shows the surface area of ZrP and ZrP with different MOF layers. The surface area of support material that is ZrP is 35 m^2/g . After deposition of two layers of MOF, the pores of ZrP are covered by MOF so the surface area is reduced to 23.75 m^2/g as shown in Figure 2d. Further deposition of MOF layers resulted in increase in surface area from 71.62 m^2/g for MOF-ZrP with 4 layers to 285 m^2/g for MOF-ZrP with 10 layers.

2.1. DFT Study of HKUST-1

The cell structure of HKUST-1, shown in Figure 3, was used to study the chemical bonding and electronic properties. The calculations for the chemical bonding and electronic properties of the HKUST-1 have been performed using full potential linearized augmented plan waves (FPLAPW) methods [25] in the frame work of DFT using WEIN2K code [26]. The exchange-correlation energies for all the systems are treated by generalized gradient approximation (GGA-sol) [27]. In FPLAPW technique the unit cell is separated in to two regions, the interstitial regions and the muffin-tin spheres region taking the muffin-tin radii (RMT) such that no charge leakages occur. Inside the muffin-tin spheres the wave function is expended in the spherical harmonics by taking $l_{\text{max}} = 10$ the maximum value of angular momentum and the magnitude of the largest vector in the charge density Fourier expansion is $G_{\text{max}} = 12 \text{ Ry}^{1/2}$. Whereas outside the sphere (interstitial region) it is expanded in plane

wave basis and cut-off value of $K_{\max} = 6/R_{\text{MT}}$ is taken. The convergence is ensured for less than 1 mRy/a.u. and 1000 k-points is used in the irreducible part of the Brillouin zone.

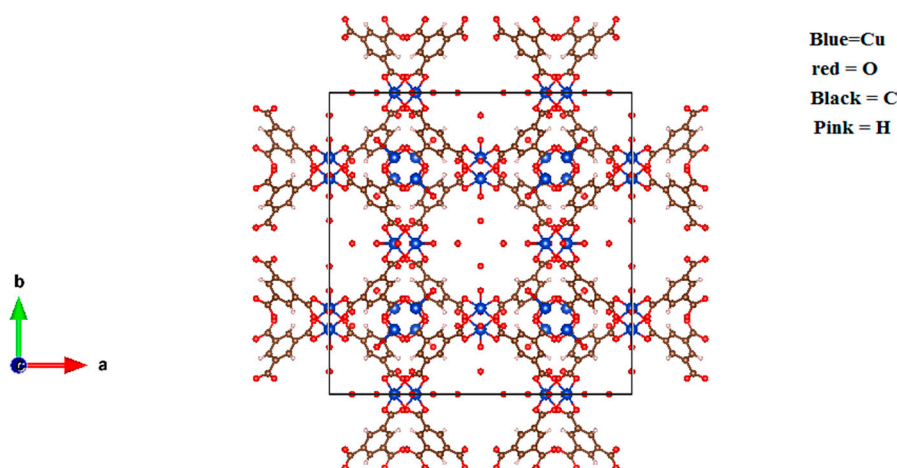


Figure 3. Structure of HKUST-1.

Chemical bonding between the constituent elements in HKUST-1 is visualized through electron charge density for the (100) and (110) crystallographic plane, as shown in Figure 4. The figure shows that there is a covalent bond between the Cu and O, due to overlapping of charge densities in both (100) and (110) plane. The charge density of OW is spherical, which confirms the ionic bond between OW and Cu atom in the (100) plane while the bond between C and H atom is also covalent, shown in the (110) plane. On the other hand, electro-negativity of the H, C, O and Cu are 2.20, 2.55, 3.44 and 1.90 (Puling scale) [28,29] respectively whose electronegative difference is 0.35 and 1.54 less than 1.67 [30] also confirms covalent bond between C-H and Cu-O.

Most of the physical properties of a compound are either directly or indirectly related with the electronic band structures. Different compounds have different kinds of band structures, due to which every compound has unique electronic properties. The electronic band structure dispersion in K-space along the high symmetry direction in the irreducible Brillouin Zone, are calculated using self-consistent field (SCF) calculations and plotted in Figure 5. The figure shows that the valance band maxima is pulled by the conduction band minima to cross the Fermi level makes the material metallic. This metallicity in the materials is due to the hybridization between Cu via O and covalent bond between H-C as in SrFeO_3 : Co [30].

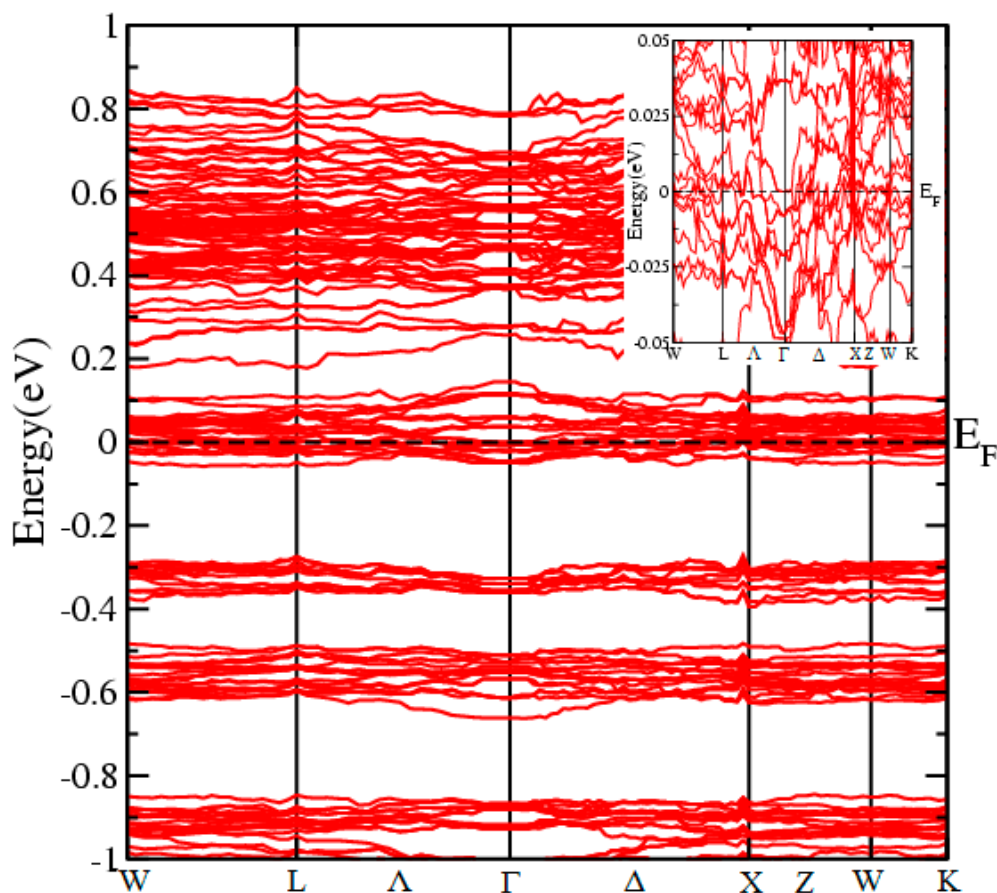


Figure 4. Electronic band structure of the HKUST-1.

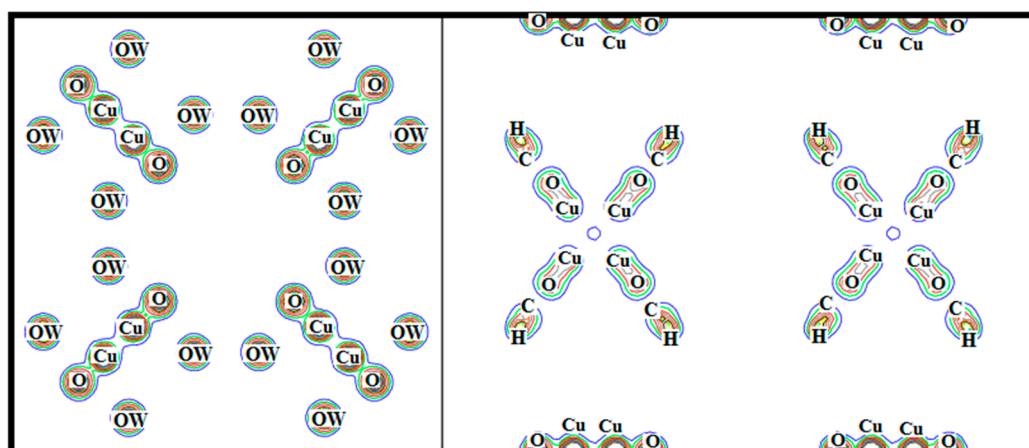


Figure 5. Electron charge densities of the HKUST-1 in (100) and in (110) crystallographic directions.

2.2. Oxidation of Cyclohexene

Figure 6 shows the product distribution and % conversion as the function of different number of layers of MOF-ZrP under the experimental conditions: 10 mL cyclohexene with 100 mg of catalyst at 80 °C in 24 h under oxygen atmosphere. Aerobic oxidation of cyclohexene in solvent free condition yielded 2-cyclohexene-1-ol and 2-cyclohexene-1-one and also cyclohexene oxide while other minor products, such as cyclohexene dimer, cyclohexanol and cyclohexanone were also detected as reported elsewhere for Cu catalysts [2,31]. Cyclohexene oxide formation is a minor reaction resulting from oxidation of C=C bond while the allylic oxidation product, 2-cyclohexen-1-one, was dominant in all

the reactions. The selectivity towards cyclohexanone was 53.6%, 44.5%, 64.9%, 35.8% and 47.9% with 2, 4, 6, 8 and 10 layers of MOF-ZrP, respectively. Similarly, the selectivity towards cyclohexanol was 41.1%, 39.1%, 32.9%, 35.3% and 41.6% respectively. In our case the high % conversion (93.7% and 93.6%) was observed with 2 and 6 layers of MOF-ZrP. Although the product distribution shows much fluctuation with the layers of MOF. Figure 6 reflects that the selectivity of catalysts towards major products with ten layers of MOF was higher as compared to others where only 0.7% by-products were formed. Selectivity is very difficult for oxidation of cyclohexene, due to the existence of two active sites, the allylic C-H bond and C=C bond. When C=C bond is oxidized, cyclohexene oxide, cyclohexanol, cyclohexanone and cyclohexanediol will be produced. As the C-H bond is oxidized, 2-cyclohexene-1-ol, 2-cyclohexene-1-one and cyclohexene hydroperoxide will be formed [3]. It was observed that the abstraction of allylic hydrogen to give allylic oxidation products is more favorable with Cu-MOF catalyst as compared to the oxidation of C=C bond as reported elsewhere [4]. No doubt, MOF-ZrP proved excellent catalytic activity for cyclohexene oxidation, but we did not observed any catalytic activity for oxidation of cyclohexane and cycloheptane at the same set of reaction parameters.

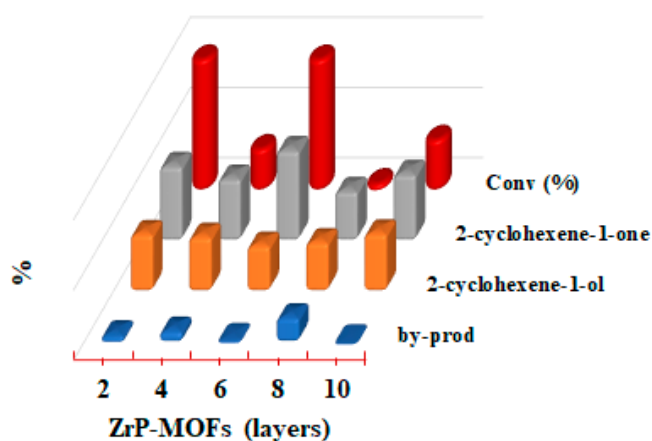


Figure 6. Conversion (%) and product distribution (%) with different layers of MOF-ZrP.

3. Experimental

3.1. Synthesis of Zirconium Phosphate by Reflux Method

Zirconyl chloride (10 g) was dispersed in 200 mL phosphoric acid solution (6 M) in a round bottom flask equipped with a condenser and a magnetic stirrer. The reaction mixture was stirred for 8 h at 90 °C. The product was washed with distilled water and dried in oven at 65 °C.

3.2. Sodium Ion Exchange

As prepared zirconium phosphate was dispersed in 0.5 N solution of sodium nitrate. The ZrP/NaNO₃ suspension was titrated against 0.1 N NaOH and 0.1 N NaNO₃ solutions in 1:1 ratio with vigorous stirring. The mixture was stirred for 12 h when the pH of the reaction mixture was maintained at 8 (constant). The product (Na-ZrP) was washed with distilled water and dried in oven at 60 °C for 24 h.

3.3. Synthesis of HKUST-1 on the Surface of ZrP

6 g of NaZrP was dispersed in 100 mL of ethanol in a round bottom flask. Copper acetate (0.307 mg) solution was added to the NaZrP suspension and stirred for 30 min at 30 °C. The product was washed with ethanol several times to remove the unreacted metal precursor. The same product was again dispersed in ethanol and stoichiometric amount of trimesic acid (Benzene 1,3,5-tricarboxylic acid) was added into it and stirred for 30 min at 30 °C. The product (HKUST-1/ZrP) was washed with ethanol and dried. One layer of MOF (HKUST-1) deposition on the surface of NaZrP is complete. For more layers, the same process was repeated [24].

3.4. Characterization of the HKUST-1/ZrP

Scanning electron microscope (SEM) of the samples was performed by using JEOL JSM-7500F (FE-SEM). PXRD patterns were recorded with Bruker-AXS D8 short arm diffractometer. TGA was performed on a TGA Q500 TA instrument. BET surface area of the samples was determined using Micromeritics ASAP 2420 with extra pure gases. FTIR spectra were recorded with Prestige 21 Shimadzu Japan in the range 500–4000 cm^{-1} .

3.5. Catalytic Test of Zirconium Phosphate Supported HKUST-1

The as prepared samples were used as a catalyst for oxidation of cyclohexene, cyclohexane and cycloheptane. Reactant(s) 10 mL and MOF-ZrP (0.1 g) were charged in a 50 mL three necked round bottom flask equipped with water circulator ($T = 3\text{ }^{\circ}\text{C}$) and magnetic stirrer. An oxygen balloon with sufficient amount of oxygen was used for oxidation. The reaction temperature was $80\text{ }^{\circ}\text{C}$. All the reactions were carried out for 24 h in order to check the catalytic activity of MOF-ZrP for each substrate oxidation. Reactant and catalyst were separated from reaction mixture and sealed in air tight vials. The products were analyzed by GC-MS.

4. Conclusions

The surface grafted MOF was successfully synthesized via layer by layer growth of MOF on ZrP, which shows prominent porosity, high surface area and good catalytic activity for cyclohexene oxidation. The major products for cyclohexene oxidation with oxygen at mild reaction conditions were cyclohexenol and cyclohexenone with less than one percent by products. DFT studies confirmed that the copper present on the edges of the MOF is responsible for the oxidation of cyclohexene. These active sites (Cu^{2+}) disappeared on dehydrating the MOF with loss of the catalytic activity for oxidation of cyclohexene. Further the increase of layers of MOF on the ZrP facilitate the mobility of electrons that enhances the catalytic activity of the catalyst with progressive growth of layers.

Author Contributions: R.A. carried out the research, A.C. was the PI of the project, M.S. wrote the initial draft and Z.A. performed the computational studies.

Funding: This research was funded by Zs Pharma under project # 213510-00071.

Acknowledgments: Authors greatly acknowledge the financial support from HEC, Pakistan under IRSIP and Texas A&M University under the project #213510-00071, Zs Pharma. We are thankful to Hong-Cai Zhou for providing BET analysis facility. We are also thankful to Johnathan Burns, Aida Contreras and Xhuezen Wang for fruitful discussions and suggestions.

Conflicts of Interest: The authors declare no conflict of interest.

References

1. Tong, J.; Wang, W.; Su, L.; Li, Q.; Liu, F.; Ma, W.; Lei, Z.; Bo, L. Highly selective oxidation of cyclohexene to 2-cyclohexene-1-one over polyoxometalate/metal-organic framework hybrids with greatly improved performances. *Catal. Sci. Technol.* **2017**, *7*, 222–230. [[CrossRef](#)]
2. Matar, S.; Hatch, L.F. *Chemistry of Petrochemical Processes*, 2nd ed.; Gulf Professional Publishing: Oxford, UK, 2000; p. 60.
3. Kouw, C.B.; Li, H.X.; Dartt, C.B.; Davis, M.E. Selective Oxidation of Alkanes, Alkenes and Phenols with Aqueous H_2O_2 on Titanium Silicate Molecular Sieves. *ACS Symp. Ser.* **1993**, *523*, 273–280. [[CrossRef](#)]
4. Fu, Y.; Su, D.; Qin, M.; Huang, R.; Li, Z. Cu(II)-and Co(II)-containing metal-organic frameworks (MOFs) as catalysts for cyclohexene oxidation with oxygen under solvent-free conditions. *RSC Adv.* **2012**, *2*, 3309–3314. [[CrossRef](#)]
5. Liu, T.; Cheng, H.; Lin, W.; Zhang, C.; Yu, Y.; Zhao, F. Aerobic Catalytic Oxidation of Cyclohexene over TiZrCo Catalysts. *Catalysts* **2016**, *6*, 24. [[CrossRef](#)]
6. Cao, Y.; Yu, H.; Peng, F.; Wang, H. Selective Allylic Oxidation of Cyclohexene Catalyzed by Nitrogen Doped Carbon Nanotubes. *ACS Catal.* **2014**, *4*, 1617–1625. [[CrossRef](#)]

7. Liu, Y.Y.; Leus, K.; Bogaerts, T.; Hemelsoet, K.; Bruneel, E.; Speybroeck, V.V.; Voort, P.V. Bimetallic–Organic Framework as a Zero-Leaching Catalyst in the Aerobic Oxidation of Cyclohexene. *ChemCatChem* **2013**, *5*, 3657–3664. [[CrossRef](#)]
8. Boudjema, S.; Rabaha, H.; Brahama, A.C. Oxidation of Cyclohexene with H₂O₂ Catalyzed by Vanadium Based Polyoxometalates Doped Modified Clays as Green Catalysts. *Acta Phys. Pol. A* **2017**, *132*. [[CrossRef](#)]
9. Junghans, U.; Kobalz, M.; Erhart, O.; Preibler, H.; Lincke, J.; Mollmer, J.; Krautscheid, H.; Glaser, R. A Series of Robust Copper-Based Triazolyl Isophthalate MOFs: Impact of Linker Functionalization on Gas Sorption and Catalytic Activity. *Materials* **2017**, *10*, 338. [[CrossRef](#)] [[PubMed](#)]
10. Farzaneh, F.; Hamidipour, L. Mn-Metal Organic Framework as Heterogenous Catalyst for Oxidation of Alkanes and Alkenes. *J. Sci. Islam. Repub. Iran* **2016**, *27*, 31–37.
11. Yopez, R.; Garcia, S.; Schachat, P.; Sanchez, M.S.; Gonzalez-Estefan, J.H.; Gonzalez-Zamora, E.; Ibarra, I.A.; Aguillar-Pliego, J. Catalytic activity of HKUST-1 in the oxidation of trans-ferulic acid to vanillin. *New J. Chem.* **2015**, *39*, 5112–5115. [[CrossRef](#)]
12. Toyao, T.; Miyahara, K.; Fujiwaki, M.; Kim, T.H.; Dohshi, S.; Horiuchi, Y.; Matsuoka, M. Immobilization of Cu Complex into Zr-based MOF with Bipyridine Units for Heterogeneous Selective Oxidation. *J. Phys. Chem.* **2015**, *119*, 8131–8137. [[CrossRef](#)]
13. Toyao, T.; Styles, M.J.; Yago, T.; Sadiq, M.M.; Riccò, R.; Suzuki, K.; Horiuchi, Y.; Takahashi, M.; Matsuoka, M.; Falcaro, P. Fe₃O₄@HKUST-1 and Pd/Fe₃O₄@HKUST-1 as magnetically recyclable catalysts prepared via conversion from a Cu-based ceramic. *CrystEngComm* **2017**, *19*, 4201–4210. [[CrossRef](#)]
14. Zhao, J.; Wang, W.; Tang, H.; Ramella, D.; Luan, Y. Modification of Cu²⁺ into Zr-based metal–organic framework (MOF) with carboxylic units as an efficient heterogeneous catalyst for aerobic epoxidation of olefins. *Mol. Catal.* **2018**, *456*, 57–64. [[CrossRef](#)]
15. Bellezza, F.; Cipiciani, A.; Constantino, U.; Negozio, M.E. Zirconium Phosphate and Modified Zirconium Phosphates as Support of Lipase. Preparation of Composites and Activity of the Supported Enzyme. *Langmuir* **2002**, *18*, 8737–8742. [[CrossRef](#)]
16. Stynes, J.A.; Clearfield, A. The preparation of Crystalline Zirconium Phosphate and Some Observations on Its Ion Exchange Behaviour. *J. Inorg. Nucl. Chem.* **1964**, *26*, 117–129.
17. Clearfield, A.; Duax, W.L.; Medina, A.S.; Smith, G.D.; Thomas, J.R. Mechanism of ion exchange in crystalline zirconium phosphates. I. Sodium ion exchange of alpha zirconium phosphate. *J. Phys. Chem.* **1969**, *73*, 3424–3430. [[CrossRef](#)]
18. Zhang, Y.; Xie, W.; Lu, X.; Wang, X.; Xu, S.; Lei, X. Preparation of microspherical α -zirconium phosphate catalysts for conversion of fatty acid methyl esters to monoethanolamides. *J. Colloid Interface Sci.* **2010**, *349*, 571–577. [[CrossRef](#)] [[PubMed](#)]
19. Cheng, S.; Clearfield, A. Oxidation of ethylene catalyzed by silver supported on zirconium phosphate: Particle size and support effect. *J. Catal.* **1985**, *94*, 455–467. [[CrossRef](#)]
20. Tuteja, J.; Choudhary, H.; Nishimura, S.; Ebitani, K. Direct Synthesis of 1,6-Hexanediol from HMF over a Heterogeneous Pd/ZrP Catalyst using Formic Acid as Hydrogen Source. *ChemSusChem* **2014**, *7*, 96–100. [[CrossRef](#)] [[PubMed](#)]
21. Sinhamahapatra, A.; Sutradhar, N.; Pahari, S.K.; Pal, P.; Bajaj, H.C.; Jayachandran, M.; Panda, A.B. Allylic and Benzylic Oxidation over CrIII-Incorporated Mesoporous Zirconium Phosphate with 100% Selectivity. *ChemCatChem* **2011**, *3*, 1447–1450. [[CrossRef](#)]
22. Khare, S.; Chokhare, R. Synthesis, characterization and catalytic activity of Fe(Salen)intercalated zirconium phosphate for the oxidation of cyclohexene. *J. Mol. Catal. A Chem.* **2011**, *344*, 83–92. [[CrossRef](#)]
23. Khare, S.; Chokhare, R. Oxidation of cyclohexene catalyzed by Cu(Salen)intercalated zirconium phosphate using dry tert-butylhydroperoxide. *J. Mol. Catal. A Chem.* **2012**, *353–354*, 138–147. [[CrossRef](#)]
24. Kan, Y.; Clearfield, A. Zirconium Phosphate Supported MOF Nanoplatelets. *Inorg. Chem.* **2016**, *55*, 5634–5639. [[CrossRef](#)] [[PubMed](#)]
25. Blaha, P.; Schwarz, K.; Luitz, J. *A Full Potential Linearized Augmented Plane Wave Package for Calculating Crystal Properties*; Technical University Wien: Vienna, Austria, 2001; ISBN 3-9501031-0-4.
26. Blaha, P.; Schwarz, K.; Madsen, G.K.H.; Kvasnicka, D.; Luitz, J. *WIEN2K: An Augmented Plane Wave + Local Orbital Program for Calculating Crystal Properties*; Technische Universität Wien: Vienna, Austria, 2013.

27. Perdew, J.P.; Ruzsinszky, A.; Csonka, G.I.; Vydrov, O.A.; Scuseria, G.E.; Constantin, L.A.; Zhou, X.; Burke, K. Restoring the Density-Gradient Expansion for Exchange in Solids and Surfaces. *Phys. Rev. Lett.* **2008**, *100*, 136406. [[CrossRef](#)] [[PubMed](#)]
28. Pauling, L. *The Nature of the Chemical Bond*, 3rd ed.; Cornell University Press: Ithaca, NY, USA, 1960.
29. Pauling, L. *The Chemical Bond*; Cornell University Press: Ithaca, NY, USA, 1967.
30. Mehmood, S.; Ali, Z.; Khan, I.; Ahmad, I. Effects of Cobalt Substitution on the Physical Properties of the Perovskite Strontium Ferrite. *Mater. Chem. Phys.* **2017**, *196*, 222–228. [[CrossRef](#)]
31. Jiang, D.; Mallat, T.; Meier, D.M.; Urakawa, A.; Baiker, A. Copper metal-organic framework: Structure and activity in the allylic oxidation of cyclohexene with molecular oxygen. *J. Catal.* **2010**, *270*, 26–33. [[CrossRef](#)]



© 2018 by the authors. Licensee MDPI, Basel, Switzerland. This article is an open access article distributed under the terms and conditions of the Creative Commons Attribution (CC BY) license (<http://creativecommons.org/licenses/by/4.0/>).